Radar sensitivity to human heartbeats and respiration

Øyvind Aardal[a], Sverre Brovoll[a], Yoann Paichard[a], Tor Berger[a], Tor Sverre Lande[b] and Svein-Erik Hamran[ab]

[a]Forsvarets forskningsinstitutt (FFI), P.O. Box 25, 2027 Kjeller, Norway;
[b]Department of Informatics at the University of Oslo, P.O. Box 1080 Blindern, 0316 Oslo, Norway.

ABSTRACT

Human heartbeats and respiration can be detected from a distance using radar. This can be used for medical applications and human being detection. It is useful to have a system independent measure of how detectable the vital signs are. In radar applications, the Radar Cross Section (RCS) is normally used to characterize the detectability of an object. Since the human vital signs are seen by the radar as movements of the torso, the modulations in the person RCS can be used as a system independent measure of the vital signs detectability.

In this paper, measurements of persons seated in an anechoic chamber are presented. The measurements were calibrated using empty room and a metallic calibration sphere. A narrowband radar operating at frequencies from 500 MHz to 18 GHz in discrete steps was used. A turntable provided measurements at precise aspect angles all around the person under test.

In an I & Q receiver, the heartbeat and respiration modulation is a combination of amplitude and phase mod- modulations. The measurements were filtered, leaving the modulations from the vital signs in the radar recordings. The procedure for RCS computation was applied to these filtered data, capturing the complex signatures. It was found that both the heartbeat and respiration detectability increase with increasing frequency. The heartbeat signatures are almost equal from the front and the back, while being almost undetectable from the sides of the person. The respiration signatures are slightly higher from the front than from the back, and smaller from the sides.

The signature measurements presented in this paper provide an objective system independent measure of the detectability of human vital signs as a function of frequency and aspect angle. These measures are useful for example in system design and in assessing real measurement scenarios.

Keywords: Radar, Radar Cross Section, heartbeats, medical radar, respiration

1. INTRODUCTION

Monitoring the heartbeats and respiration of human beings from a distance is possible with radar technology. It is the small movements connected to the breathing and heartbeats that are detected by the radar.[1] They are sensed through small variations in the received echo of the radar's transmitted electromagnetic signals. It has potential applications in medicine for patient monitoring,[2] sleep apnea detection[3] , heart rate variability (HRV) measurement[4] and for quick contact-less measurements of a person's vital signs. Other possible applications are in surveillance and security, through the wall detection of people[5] and detection of people buried under collapsed buildings, ground or snow.[6]

Over the years, different radar technologies operating with a few hundred MHz[7] to over two hundred GHz[8] have been used to detect human heartbeats and respiration. While many systems have been developed for this purpose, which frequencies to use and from which angle of incidence have not been given much attention. In[9] it was found that a person lying down has a larger radar cross section (RCS) of the cardiopulmonary activity from the back than from the front. In[10] the breathing cross section on a person lying down from various angles using an ultra wide band (UWB) radar with center frequency 750 MHz was calculated. The breathing response was found strongest when the person was lying sideways facing the antenna. In[11] the RCS of the human heartbeat and respiration was found in the 500 MHz to 3 GHz range using an UWB radar, revealing an increase of vital signs response with increased frequency. Antennas can also be attached to the chest surface to detect reflections from the heart wall instead of the chest surface. In this case, it was found in[12] that lower frequencies are best because of the lowered attenuation with frequency.

Further author information: E-mail:oyvind.aardal@ffi.no, Telephone: +4763807041.

Dette er en postprint-versjon/This is a postprint version.
DOI til publisert versjon/DOI to published version: 10.1117/12.2180924

Finding the optimal way to detect heartbeats and respiration using radar depends on the application. The optimal method for detecting the heartbeat rate is not necessarily the same as the optimal way to detect a certain heart disease. In this paper, the optimal setup for vital signs detection is defined as the setup where the vital signs are most visible in the radar recording thus maximizing their probability of detection. There are many variables affecting the detectability of heartbeats and respiration with radar. They include which person is under test, posture, angle of incidence, transmitted frequency, the surroundings, respiratory pattern and heart condition. This study is limited to investigating the dependence on frequency and angle when the person is in a normal seated position.

In this paper the optimal frequencies and aspect angles for remote heartbeat and respiration detection were investigated. Calibration of the radar recordings were performed to remove instrument and environment dependence. A robust measure for quantizing the recorded modulation in the measurements was used. The results were normalized to calibrated measurements on human beings using frequencies in the 500 MHz - 18 GHz range.

2. BACKGROUND ON RCS AND BODY MOVEMENTS

In a typical radar measurement with an I & Q receiver, the measurement consists of data in the complex plane which can be described by an amplitude component and a phase component. Every object within the antenna beam will contribute to the total received signal, which is a sum of all the backscattered echos. A measurement of a moving point target in the presence of stationary objects can be described by

$$b(t) = A_s e^{i\phi_s} + A_m e^{i\phi_m(t)}, \tag{1}$$

$$A_m = \frac{A_r\sqrt{\sigma}}{4\pi R_m(t)^2}, \tag{2}$$

$$\phi_m(t) = \frac{2\omega_c R_m(t)}{c}. \tag{3}$$

In the above equation, $A_s e^{i\phi_s}$ is the sum of the echos from the stationary targets in the scene, with A_s being the amplitude and ϕ_s the phase of the sum. As long as the objects remain stationary, their contribution to the radar recording remain the same even if there is a lot of complexity in the scene. A_m is the amplitude of the echo from the moving target, and is dependent on both the radar system contributions to the amplitude A_r, the object's RCS σ, and the time varying range R_m to the object. The phase ϕ_m is directly coupled to the system center frequency ω_c, the range R_m and the speed of electromagnetic wave propagation c in the medium of propagation. An illustration is shown in Figure 1.

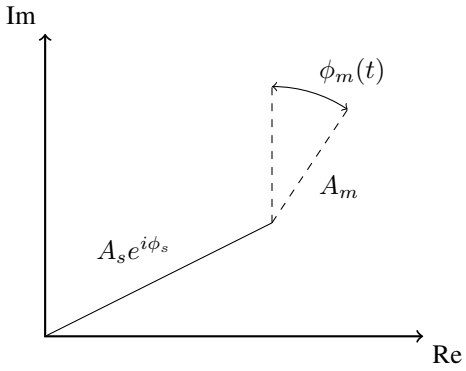

Figure 1. The signal in the complex plane in the simple scenario of one moving point scatterer and a sum of stationary scatterers.

More moving point targets at slightly different distances can be introduced to (1). In this case, the total signal $b(t)$ does not follow a circle segment in the complex plane but has a more complex shape. In a real life measurement of the human chest this is a more realistic model than the single point scatterer model of (1).[13] Moving parts of the torso at different distances from the radar will all act as moving reflectors. Each individual reflector contributes a phase modulation with different phase offsets and amplitudes to the total radar recording. Thus, a radar heartbeat or respiration recording does not look like a clean arc as seen in Figure 1, but is deformed.

Dette er en postprint-versjon/This is a postprint version.
DOI til publisert versjon/DOI to published version: 10.1117/12.2180924

Even though the chest movements connected to the heartbeat are much smaller than the wavelength λ, they can be detected through the phase variations. The restricting factors on the heartbeat detection are noise and other movements in the scene such as small body movements.

The most common measure of how well an object reflects incident radar waves is the radar cross section. The definition of RCS as given by[14] is

$$RCS = \lim_{R\to\infty} 4\pi R^2 \frac{|E_r^2|}{|E_i^2|}, \tag{4}$$

where E_r is the electric field strength of the scattered wave at the radar, E_i is the electric field strength of the incident wave on the target and R is the range from the radar to the target. By definition, the RCS is the amount of incident radar power an object will reflect as a function of frequency and aspect angle. It is a measure independent from range and radar system characteristics.

In a typical radar measurement, echos from all objects within the antenna beam will contribute to the signals. In addition, the received signal is dependent on the radar system characteristics such as the transmitted power and antenna gain. When measuring the RCS of an object, all of these components need to be removed. The use of echo free rooms can reduce the amount of background clutter reflections, but the attenuation may be insufficient for measuring small targets. A good approach finding the RCS of an object is to use three measurements steps. First, the object under test is measured. Second, a calibration object with known RCS such as a sphere, a flat plate or a corner reflector is placed in the same spot as the the object was placed. Last, an empty scene measurement is performed and subtracted from the other two. The object measurement can then be divided by the calibration object measurement, outputting the RCS of the object.

The approach sketched above for finding the RCS works for a stationary target, but what if the target is moving? In (1) and Figure 1 it is seen that a moving point target follows an arc in the complex plane. If the target moves a distance $\Delta R_m > \frac{\pi c}{\omega_c}$, this will look like a circle segment centered around $A_s e^{i\phi_s}$. If the system contribution A_r is known, σ can be estimated from this arc in the complex plane, which was done in[9] and.[15]

A straight forward RCS measurement of a person will result in just that; the RCS of the person, but not of the vital signs. A better solution would be to estimate the phase $\phi_m(t)$ of the moving chest and characterizing it through for instance the phase modulation index $h = \Delta\phi_m$, where $\Delta\phi_m$ is the peak deviation from the mean phase.

In[11] the movement of the chest was estimated under the assumption that the modulation follows an arc such as the one seen in Figure 1. It was found that although estimates can be found, they are not accurate. The estimated chest movement from a heartbeat was found to vary between 0.5 and 1 mm. The reason for this is that the shape of the heartbeat in the complex plane does not follow a simple circle segment-like arc as in Figure 1, but has a more complex form. In[11] this is explained by the chest not being a point scatterer but a continuum of scatterers of slightly different ranges from the radar. An example heartbeat recording can be seen in Figure 2. It is clear that this is not a circle segment, but a more complex shape complying with the many point models of[11] and.[13] This shape does not remain exactly the same from measurement to measurement, and also changes with frequency. A measure of modulation based on the estimation of the phase deviation in such a signal is not accurate, and estimation errors could very well be larger than the actual variations of the modulation index. Thus, using the phase modulation index for quantizing which frequencies and angles are optimal is not viable.

A robust method for estimating the size of the modulations is needed, as none of the standard methods discussed so far are adequate. The measure should get the correct size of the modulation, even though its shape is different from one measurement to the next. In the following an improved modulation extraction method is proposed for robust extraction of both heartbeats and breathing. This method was used for quantizing the vital sings as a function of frequency and aspect angle.

3. MEASUREMENTS AND METHODOLOGY

All measurements were conducted on two male subjects age 26 and 32 in an anechoic chamber using a vector network analyzer[16] as a radar. The transmitted signals were single frequency continuous waves with an IF bandwidth of 100 Hz which were sampled at 113 Hz sampling frequency. Two different antennas were used, a Vivaldi antenna with a 28 cm opening for the 0.5-4 GHz range and a wide-band horn antenna of 4.1 $\times$ 4.1 cm for the 4-18 GHz range. Measurements at 4

Dette er en postprint-versjon/This is a postprint version.
DOI til publisert versjon/DOI to published version: 10.1117/12.2180924

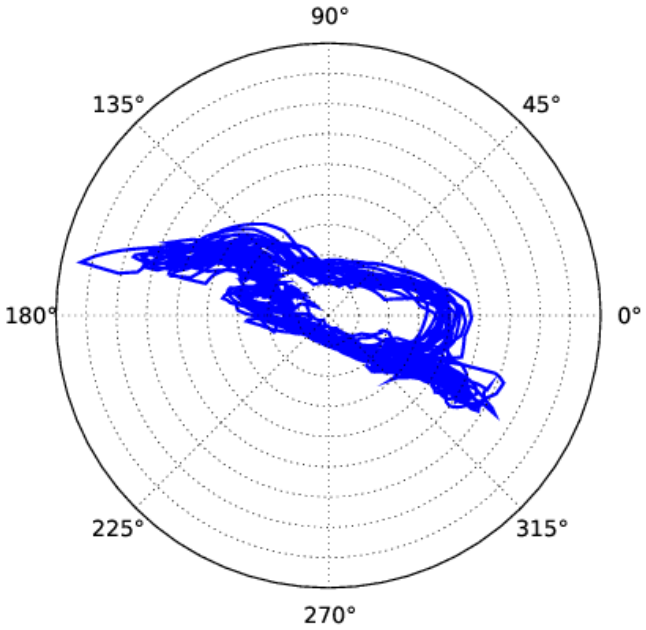

Figure 2. A 2 GHz CW recording of several heartbeats seen in the complex plane. The axes are linear scale, with voltage along the radial axis. The measurements are from a person lying down holding his breath. Here the mean has been subtracted from the data so that the modulation is seen clearer.

GHz were conducted both with the low frequency and with the high frequency antenna. The measurements were compared to ensure consistent results.

In the 500 MHz to 4 GHz range, measurements were conducted in 500 MHz steps, while 1 GHz steps were used for 4-18 GHz. The person was seated in the same position on a chair for all measurements. The chair was placed on a turntable electronically controlled from a computer. With the turntable, accurate steps of 30° were made from 0 to 360°. In Figure 3 the measurement setup is indicated. This way radar recordings were made of the person from aspect angles all around the body. For each person, angle and frequency measurements of the person were recorded both with normal breathing and with the person holding his breath.

In the following a suitable measure of physiological modulations due to breathing and heart beats is explained. This measure is termed the heartbeat or respiration modulation signal (M) in units m^2, which is the same unit as RCS.

When doing ranged radar heartbeat recordings, there are three main parameters to be varied. These are the transmitting frequency of the radar, the aspect angle of the radar to the person and the range between the person and the antennas. The distance from the antenna to the person determines whether the person can be considered to be in the near field or far field of the antenna, which parts of the person is in the main beam, the amount of clutter reflections received and the attenuation from the two way travel of the EM field.

In[17] and[18] the methodology for finding the physiological modulation signal through calibrated wide-band measurements is given. A summary of the procedure for single frequency measurements is given here, for a thorough introduction to the calibration procedure the reader is referred to the referenced papers or more general sources on calibrated radar recordings and RCS.[19,20]

The measurements were conducted on slightly different ranges between the persons, with the smallest distance between the person and the antenna being $R = 131$ cm. The lowest frequency transmitted was at 500 MHz Tx, which gives a wavelength of $\lambda = 60$ cm. In this case $R > 2\lambda$, which means all the measurements were conducted in the far field. However, above 3GHz, the Vivaldi antennas were below the Fraunhofer distance of $R > \frac{2D^2}{\lambda}$ with D being the antenna size.

Dette er en postprint-versjon/This is a postprint version.
DOI til publisert versjon/DOI to published version: 10.1117/12.2180924

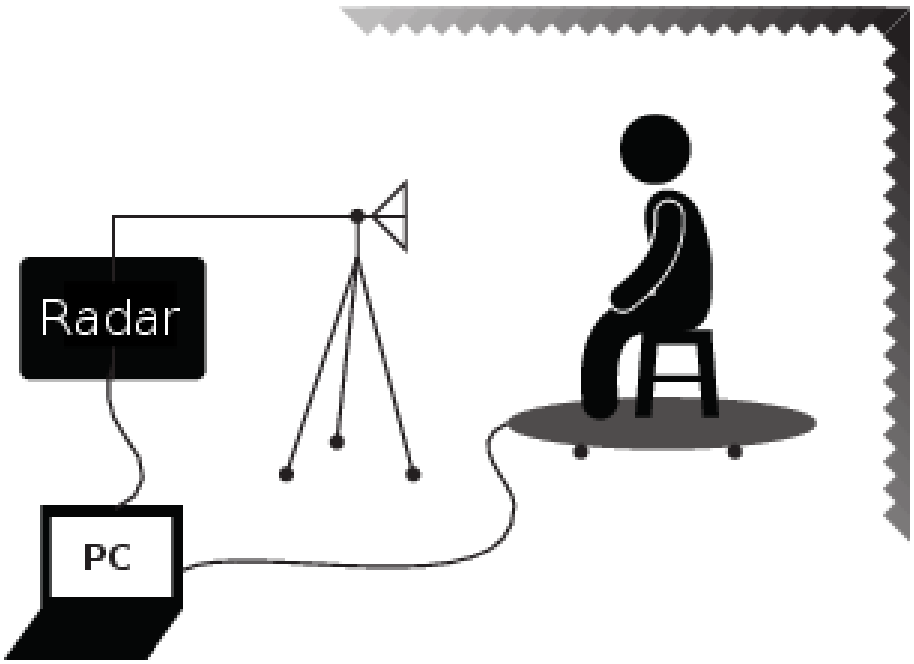

Figure 3. Measurement setup. The person was seated on a chair placed on a turntable inside an anechoic room. A network analyzer connected to a PC was used as a radar.

For each calibrated value, three measurements were carried out: 1) The person under test either breathing or holding his breath, 2) a metallic calibration sphere of known RCS placed at exactly the same distance from the antennas as the person was, and 3) the empty room. The received signal at the radar for these measurements are respectively

$$\begin{aligned} \text{person} : b_P(t) &= V_t H_a^2 (H_C + H_P(t)) && (5) \\ \text{sphere} : b_S &= V_t H_a^2 (H_C + H_S) && (6) \\ \text{empty room} : b_C &= V_t H_a^2 H_C, && (7) \end{aligned}$$

where V_t is the signal generated by the radar, H_a is the antenna transfer function, H_C is the clutter transfer function, H_S the sphere transfer function and H_P the person transfer function. From (5) - (7) a calibrated recording of the person is found:

$$\begin{aligned} b_{cal}(t) &= \frac{b_P(t) - b_C}{b_S - b_C} \\ &= \frac{H_P(t)}{H_S}. \end{aligned} \quad (8)$$

Given that the person and calibration sphere were placed the same distance R from the radar, their transfer functions are

$$H_S = \frac{1}{4\pi R^2} \frac{E_{r,S}(R,t)}{E_i(R,t)} \quad (9)$$

$$H_P = \frac{1}{4\pi R^2} \frac{E_{r,P}(R,t)}{E_i(R,t)}. \quad (10)$$

$E_{r,S}(R,t)$ and $E_{r,P}(R,t)$ are the electric field strengths of the wave scattered off the sphere and person received at the radar. $E_i(R,t)$ is the electric field strength incident on the target. This is of course a simplification, as neither the sphere nor the person is at exactly one range from the radar, but spans a small range window around R. Using (8) and (10), it is seen that the magnitude squared of the calibrated measurement is

$$|b_{cal}|^2 = \frac{RCS_P}{RCS_S}. \quad (11)$$

Dette er en postprint-versjon/This is a postprint version.
DOI til publisert versjon/DOI to published version: 10.1117/12.2180924

In (8), the calibrated recording $b_{cal}(t)$ still contains stationary reflections, drift and involuntary movements. To extract the physiological movement, a 0.5 Hz digital high-pass filter was applied to the heartbeat measurement data and a linear trend removal was applied to the respiration measurement data. The filter used was a two way zero phase IIR Chebyshev type 2 filter with a minimum 40 dB stop-band attenuation. This removes the major systematic errors of the recording, and we are left with only the physiological modulation and noise. The calibrated recording after filtering, $\hat{b}_{cal}(t)$, can now be used to find the heartbeat or respiration modulation signal:

$$M_H = |\hat{b}_{cal}|^2 RCS_S, \quad \text{using held breath data} \tag{12}$$

$$M_R = |\hat{b}_{cal}|^2 RCS_S, \quad \text{using respiration data.} \tag{13}$$

The mean values $\bar{M}_H$ and $\bar{M}_R$ of these are the heartbeat and respiration modulation signal, in units of square meters. This measure is independent of range, antennas and radar system, and describes the physiological modulation a radar detects.

It is worth noting that this approach to the calibrated measurements are similar to what is used for RCS measurements, both having units of square meters. The post processing of the data however, is different. In a RCS measurement the reflectivity of the object is found. The modulation signal on the other hand is the size of the modulation in a recording of the moving object. This means that an object with a large RCS but small movement will have a small modulation signal. M_H and M_H can be thought of as the RCS of the heartbeat and respiration movement. They are dependent on both the RCS of the moving parts of the chest and the magnitude of the motion.

4. RESULTS

The measurements were carried out on two persons, resulting in the heartbeat modulation signal M_H and the respiration modulation signal M_R as functions of both frequency f and aspect angle θ. To make the results more accessible, empirical models of the modulation signals were made. These are presented in Section 4.2, resulting in the mathematical models (15)-(18).

4.1 Measurement results

Results of the heartbeat modulation signal experiments can be seen in Figure 4 and Figure 5. Figure 4 displays the heartbeat modulation signal $\bar{M}_H$, defined in (12), as a function of aspect angle. For each angle, the mean $\bar{M}_H$ value for both persons over all the frequencies is plotted. The heartbeat is best detected from the front and the back of the person.

In Figure 5 the heartbeat modulation signal from directly in front and back aspect angles have been plotted as a function of frequency. It is seen that $\bar{M}_H$ increases with frequency. The mean heartbeat modulation signal from the front and back varies from $\bar{M}_H = 2 \cdot 10^{-6}$ m^2 at 500 MHz to $\bar{M}_H = 1.8 \cdot 10^{-3}$ m^2 at 17 GHz. For the frequency range 500 MHz to 3 GHz, similar experiments with aspect angle directly from the front is reported in[18] with similar results.

Significant variations in the modulation is seen, both between persons and with frequency. Most notable are the spike at 3 GHz for person1 and the spike at 12 GHz for person2. There are several explanations for these variations in modulation. First of all, variations with frequency are expected, as the constructive and destructive interference of the echos are frequency dependent. Other more random factors also play a part. Small changes in body posture, pulse and state of the held breath may change how much the chest moves when the heart is beating. The periodic movement of other body parts and veins pulsating with the heartbeat may also differ from measurement to measurement.

The results of the respiration modulation signal M_R is displayed in a similar fashion as the heartbeat modulation signal results in Figure 6 and Figure 7. The mean respiration modulation signal from the front and the back varies from $\bar{M}_R = 2.06 \cdot 10^{-05}$ m^2 to $\bar{M}_R = 0.199$ m^2. As expected, the respiration modulation signal is higher than the heartbeat modulation signal due to the chest movement being larger for breathing than for the heartbeat alone. From Figure 6 it is seen that the modulation in the radar recordings of respiration is sharply decreased when the aspect angle is not from the front or the back. While the respiration modulation signal is higher than the heartbeat modulation signal, it seems that the heartbeat movements are slightly more omni-directional.

In Figure 7 it is seen that the modulation from one of the persons from the back is much smaller than the other. This is explained by great individual variations between persons' respiration moving the back of the body.

Dette er en postprint-versjon/This is a postprint version.
DOI til publisert versjon/DOI to published version: 10.1117/12.2180924

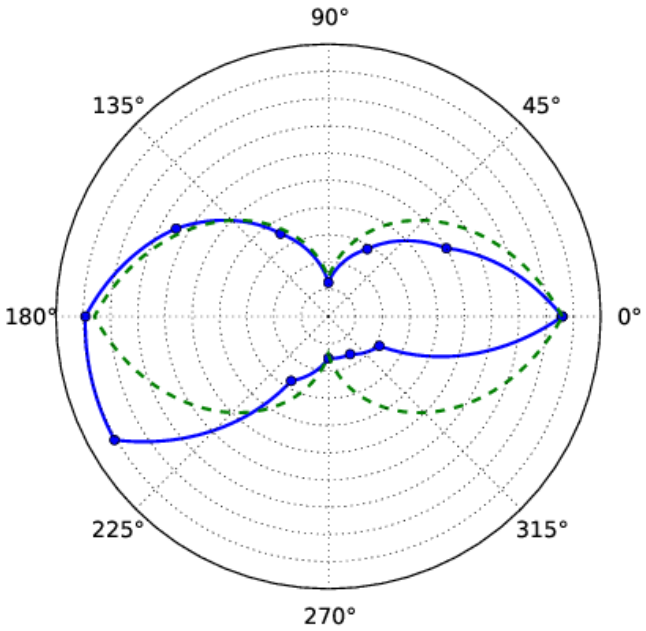

Figure 4. The heartbeat modulation signal as a function of aspect angle. With 0°, the person is facing the antenna, while with $\theta = 180^\circ$ the antenna is pointed at the back of the person. The distance from the center is the modulation signal in linear scale m^2. The heartbeat is equally well detected from the front and the back in ranged radar heartbeat measurements. The size of the observed modulation decreases from the sides. The dashed line is the empirical model of the heartbeat modulation, as defined by (16).

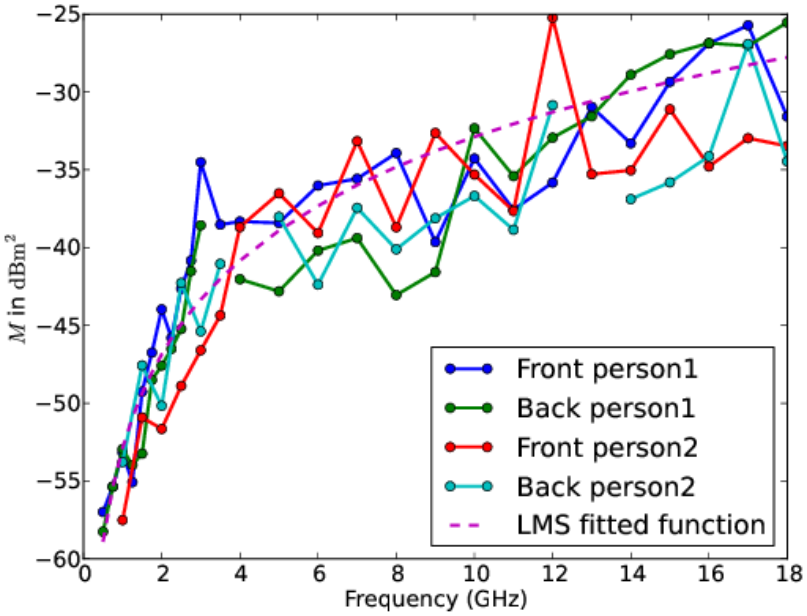

Figure 5. The heartbeat modulation signal as a function of frequency. The front and back M_H are plotted for both persons used in the experiments. The dashed line represents our empirically found model for the size of the heartbeat modulations as a function of frequency. The heartbeat modulation seen in the radar recordings increases with increasing frequency over the entire 0-18 GHz range. Note that the results are dB scale, thus the flattening of the curves with higher frequency.

Dette er en postprint-versjon/This is a postprint version.
DOI til publisert versjon/DOI to published version: 10.1117/12.2180924

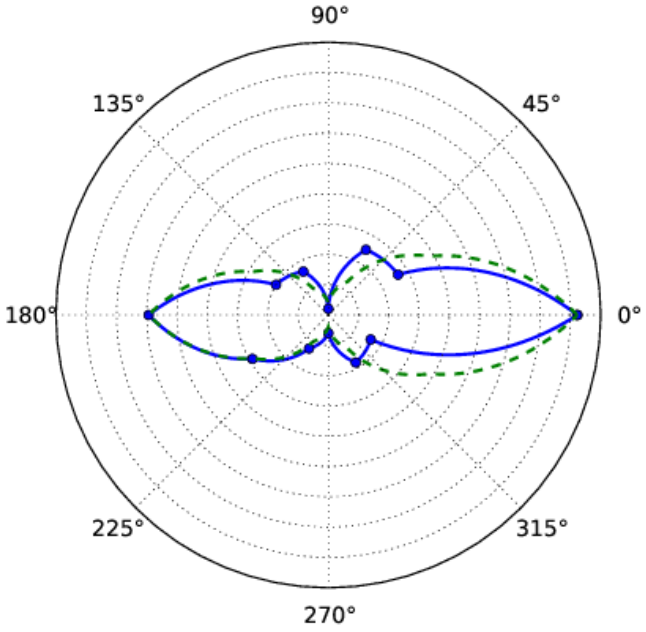

Figure 6. The respiration modulation measure as a function of aspect angle. With $\theta = 0°$, the person is facing the antenna, while with $\theta = 180°$ the antenna is pointed at the back of the person. The blue line is the mean respiration modulation signal over all the tested frequencies. The distance from the center is the modulation signal in linear scale m^2. The dashed line is the empirical model (18) of the modulation signal.

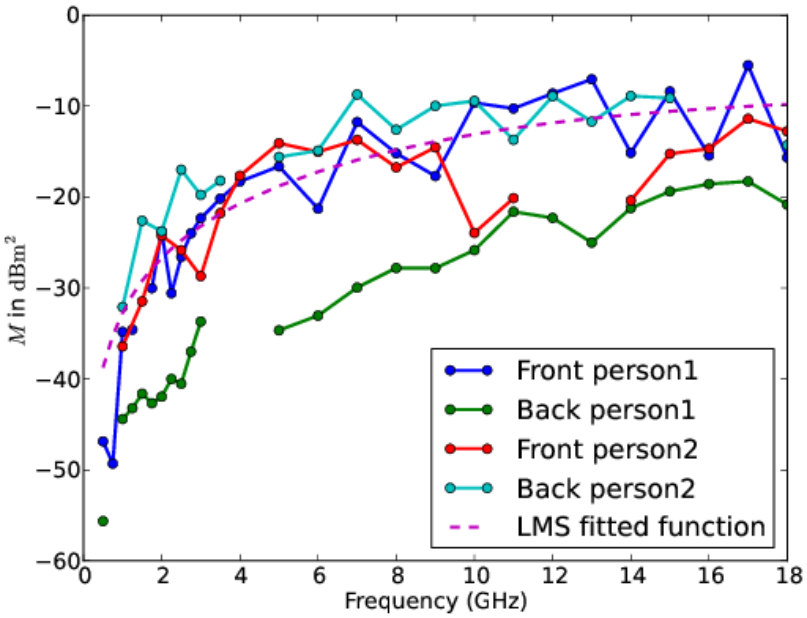

Figure 7. The respiration modulation signal as a function of frequency. The front and back M_R are plotted for both persons used in the experiments. The dashed line is the empirically found model of the respiration modulation signal. It is seen that the modulation increases with increasing frequency. In addition, there is a large difference in the observed modulation from the back between the two persons. This indicates large variations between different individuals. The gaps in the plotted data are measurements that were removed due to movement artifacts.

Dette er en postprint-versjon/This is a postprint version.
DOI til publisert versjon/DOI to published version: 10.1117/12.2180924

4.2 Empirical modulation models

The results presented in Figure 4 and Figure 5 display the measured heartbeat modulation signal as a function of angle and frequency. These results are useful when determining how well the human heartbeat can be detected in various arrangements. To make the experimental results more accessible, we have made an empirical model of the heartbeat modulation signal as a function of frequency and aspect angle.

Modelling the heartbeat modulation signal, we fitted a suitable function matching our data. A coarse approximation of the human chest seen directly from the front or the back is as a flat plate. The RCS of a flat plate is given by

$$\sigma_{plate} = \frac{4\pi A^2}{\lambda^2}, \tag{14}$$

with A being the area of the plate and $\lambda = c/f$ the wavelength. A least squares fitting of (14) to the heartbeat modulation signal shows a good fit, see Figure 5. The empirical model of the heartbeat modulation signal seen directly from the front, $M_H(f, 0)$, is:

$$M_H(f, 0) = 5.15 \cdot 10^{-24} f^2. \tag{15}$$

The angle dependency of the modulation signal follows a triangle wave-like form. $\theta = 0$ is the aspect angle directly from the front, while $\theta = \pi$ is the aspect angle directly from the back. The angular dependence model is

$$M_H(f, \theta) = \begin{cases} M_H(f,0)(1 - \frac{1.68}{\pi}|\theta|), & |\theta| \leq \frac{\pi}{2} \\ M_H(f,0)(\frac{1.68}{\pi}(|\theta| - \frac{\pi}{2}) + 0.16), & \frac{\pi}{2} \leq |\theta| \leq \pi. \end{cases} \tag{16}$$

An empirical model made from least squares curve fitting of the recorded data was made for the respiration modulation signal M_R as well. The model of M_R as a function of frequency with aspect angle from the front, as seen in Figure 7, is given by:

$$M_R(f, 0) = \frac{\arctan(5.33 \cdot 10^{-21} f^2)}{10}. \tag{17}$$

$M_R(f, \theta)$ is relatively larger from the front and back than from other angles compared to $M_H(f, \theta)$, so a more directional model of the angle dependency is chosen:

$$M_R(f, \theta) = \begin{cases} M_R(f,0)(0.95(\frac{2}{\pi}(|\theta| - \frac{\pi}{2}))^2 + 0.05), & |\theta| \leq \frac{\pi}{2} \\ M_R(f,0)(0.67(\frac{2}{\pi}(|\theta| - \frac{\pi}{2}))^2 + 0.05), & \frac{\pi}{2} \leq |\theta| \leq \pi. \end{cases} \tag{18}$$

This angle dependency model can be seen as the dashed line in Figure 6.

The large variations between the two persons suggests that the models are person dependent. Measurements on more persons are needed to provide exact models of the vital signs modulation dependency of frequency and aspect angle. The trend seen here is valid though: That the heartbeat and respiration modulation increases with increasing frequency and are best seen from the front and the back of the person.

5. DISCUSSION

The measurements show a trend of increasing radar sensitivity to vital signs with increasing frequency. This was expected, because of the increased movement relative to the wavelength. The decrease in sensitivity from the sides of the person relative to the front was also expected, as both the heartbeat and respiration movement was expected to be more pronounced from the front. More surprising was the high sensitivity to both respiration and heartbeats seen from the back of the person, which was also reported by.[21] When the heart is beating, it beats against the chest causing small surface movements. The heart could be causing small surface movements in the back in this way as well. Another explanation is that the vital signs does not only cause movements locally but causes the entire upper body to slightly move with each heartbeat and breathing

Dette er en postprint-versjon/This is a postprint version.
DOI til publisert versjon/DOI to published version: 10.1117/12.2180924

cycle. If this movement is mostly back and forth and not to the sides, it is compliant with the measured results. Third, it could also be that the movements of the back are actually smaller but that the back of these persons has a higher RCS than the front. A high RCS target with small movements and a small RCS target with larger movements are not differentiated in the method presented in this paper.

From the calibrated measurements of the heartbeat and respiration modulation signals, models for the range and frequency dependency of the modulations were made. By the definitions (12) and (13), the modulation signals will not, in theory, catch movements larger than one wavelength. In this case the movements will be seen as circles in the complex plane. The respiration modulation signal model takes this into account and will saturate with increasing frequency. The heartbeat modulation signal model on the other hand continues to increase with increasing frequency, making the model invalid for wavelengths smaller than the chest movement. Typical chest movements caused by heartbeats are in sub-millimeter size. For 18 GHz Tx frequency, the highest frequency used in this paper, the wavelength is $\lambda = 1/6 \cdot 10^{-1} \approx 1.67$ cm. This is about 20 times the size of the chest movement caused by heartbeats. From these calculations the model should be valid for Tx frequencies up to around 150 GHz.

As seen in Figure 4 to Figure 7, the recorded data indicate major variations. Individual variations in the size of the modulation from different persons are expected. Every person has a different body topology, which gives rise to differences in interference as well as scattering. Other factors that can change the size of the modulation are body posture and how hard and fast the heart is beating.

The measurements presented in this paper were conducted on only two persons. This is too few persons for this study to be an exact measure for a general population, and does not tell the expected deviation from these numbers in a general population. On the other hand, for these two persons a total number of 528 measurements were conducted divided over the frequencies and aspect angles. The trend seen in the data of increasing sensitivity with increasing frequency and best sensitivity from the front and the back should hold for a general population. It also complies with the theory that the radar records the sum of the movements of the chest surface.[1,11,13]

6. CONCLUSION

Calibrated ranged radar measurements of the human heartbeat and respiration were conducted in the range 0.5 - 18 GHz and with aspect angles all around the body. From these recordings, empirical estimators of the human heartbeat and respiration modulation were made. Both the heartbeat and respiration modulation increases with increasing frequencies, and are best observed from the front and the back. There were large differences between the two persons' recorded vital signs modulations. Empirical models were made from the data, providing a reference for the size of the recorded modulation as a function of both frequency and aspect angle. These modulation signal models are useful for computing the detection possibility in real world scenarios.

ACKNOWLEDGMENTS

This work is part of the MELODY project funded by the Research Council of Norway under contract number 187857/S10.

REFERENCES

1. Ø. Aardal, Y. Paichard, S. Brovoll, T. Berger, T. S. Lande, and S.-E. Hamran, "Physical working principles of medical radar," *Biomedical Engineering, IEEE Transactions on* **60**(4), pp. 1142–1149, 2013.
2. E. Staderini, "UWB radars in medicine," *Aerospace and Electronic Systems Magazine, IEEE* **17**, pp. 13–18, Jan 2002.
3. Y. S. Lee, P. Pathirana, C. Steinfort, and T. Caelli, "Monitoring and analysis of respiratory patterns using microwave doppler radar," *Translational Engineering in Health and Medicine, IEEE Journal of* **2**, pp. 1–12, 2014.
4. W. Massagram, N. Hafner, S. Yamada, V. Lubecke, and O. Boric-Lubecke, "Feasibility of hrv measurement from single-channel doppler radar," in *Antennas and Propagation Society International Symposium, 2007 IEEE*, pp. 269–272, June 2007.
5. N. Maaref, P. Millot, C. Pichot, and O. Picon, "A study of UWB FM-CW radar for the detection of human beings in motion inside a building," *Geoscience and Remote Sensing, IEEE Transactions on* **47**, pp. 1297–1300, May 2009.

Dette er en postprint-versjon/This is a postprint version.
DOI til publisert versjon/DOI to published version: 10.1117/12.2180924

6. K.-M. Chen and H.-R. Chuang, "Measurement of heart and breathing signals of human subjects through barriers with microwave life-detection systems," *Engineering in Medicine and Biology Society, 1988. Proceedings of the Annual International Conference of the IEEE* , pp. 1279–1280 vol.3, Nov 1988.
7. M. Jelen and E. M. Biebl, "Multi-frequency sensor for remote measurement of breath and heartbeat," *Advances in Radio Science* **4**, pp. 79–83, 2006.
8. D. Petkie, C. Benton, and E. Bryan, "Millimeter wave radar for remote measurement of vital signs," in *Radar Conference, 2009 IEEE*, pp. 1 –3, May 2009.
9. J. Kiriazi, O. Boric-Lubecke, and V. Lubecke, "Radar cross section of human cardiopulmonary activity for recumbent subject," in *Engineering in Medicine and Biology Society, 2009. EMBC 2009. Annual International Conference of the IEEE*, pp. 4808 –4811, sept. 2009.
10. A. Nezirovic, S. Tesfay, A. Valavan, and A. Yarovoy, "Experimental study on human breathing cross section using uwb impulse radar," in *Radar Conference, 2008. EuRAD 2008. European*, pp. 1 –4, oct. 2008.
11. Ø. Aardal, S.-E. Hamran, T. Berger, Y. Paichard, and T. S. Lande, "Chest movement estimation from radar modulation caused by heartbeats," in *Biomedical circuits and systems conference (BIOCAS 2011), 2011 IEEE*, pp. 452–455, IEEE, November 2011.
12. S. Brovoll, Ø. Aardal, Y. Paichard, T. Berger, T. S. Lande, and S.-E. Hamran, "Optimal frequency range for medical radar measurements of human heartbeats using body-contact radar," in *Engineering in Medicine and Biology Society (EMBC), 2013 35th Annual International Conference of the IEEE*, pp. 1752–1755, IEEE, 2013.
13. C. Li and J. Lin, "Random Body Movement Cancellation in Doppler Radar Vital Sign Detection," *Microwave Theory and Techniques, IEEE Transactions on* **56**, pp. 3143 –3152, dec. 2008.
14. M. Skolnik, ed., *Radar Handbook*, McGraaw-Hill Book Company, second ed., 1990.
15. J. E. Kiriazi, O. Boric-Lubecke, and V. M. Lubecke, "Dual-frequency technique for assessment of cardiopulmonary effective rcs and displacement," *Sensors Journal, IEEE* **12**(3), pp. 574–582, 2012.
16. "Agilent Network Analyzer N5245A PNA-X, http://www.home.agilent.com/agilent/product.jspx?nid=-536902643.898624.00&cc=NO&lc=eng."
17. Ø. Aardal, S.-E. Hamran, T. Berger, J. Hammerstad, and T. S. Lande, "Radar Cross Section of the Human Heartbeat and Respiration," in *Biomedical Circuits and Systems Conference, 2010. BioCAS 2010.*, pp. 53–57, IEEE, November 2010.
18. Ø. Aardal, S.-E. Hamran, T. Berger, J. Hammerstad, and T. S. Lande, "Radar cross section of the human heartbeat and respiration in the 500MHz to 3GHz band," in *Radio and Wireless Symposium (RWS), 2011 IEEE*, pp. 422–425, IEEE, January 2011.
19. A. Morgan, "Ultra-wideband impulse scattering measurements," *Antennas and Propagation, IEEE Transactions on* **42**, pp. 840–846, Jun 1994.
20. S. Hantscher, B. Etzlinger, A. Reisenzahn, and C. Diskus, "UWB Radar Calibration Using Wiener Filters for Spike Reduction," in *Microwave Symposium Digest, 2006. IEEE MTT-S International*, pp. 1995–1998, June 2006.
21. O. Boric-Lubecke, J. Lin, B.-K. Park, C. Li, W. Massagram, V. M. Lubecke, and A. Host-Madsen, "Battlefield triage life signs detection techniques," in *SPIE Defense and Security Symposium*, pp. 69470J–69470J, International Society for Optics and Photonics, 2008.

Dette er en postprint-versjon/This is a postprint version.
DOI til publisert versjon/DOI to published version: 10.1117/12.2180924